

# A pluripotent developmental state confers a low fidelity of chromosome segregation

Chenhui Deng,<sup>1,2</sup> Amanda Ya,<sup>1,2</sup> Duane A. Compton,<sup>1,2</sup> and Kristina M. Godek<sup>1,2,\*</sup>

<sup>1</sup>Department of Biochemistry and Cell Biology, Geisel School of Medicine at Dartmouth, Hanover, NH, USA

<sup>2</sup>Dartmouth Cancer Center, Geisel School of Medicine at Dartmouth, Lebanon, NH, USA

\*Correspondence: [kristina.m.godek@dartmouth.edu](mailto:kristina.m.godek@dartmouth.edu)

<https://doi.org/10.1016/j.stemcr.2022.12.008>

## SUMMARY

During *in vitro* propagation, human pluripotent stem cells (hPSCs) frequently become aneuploid with incorrect chromosome numbers due to mitotic chromosome segregation errors. Yet, it is not understood why hPSCs exhibit a low mitotic fidelity. Here, we investigate the mechanisms responsible for mitotic errors in hPSCs and show that the primary cause is lagging chromosomes in anaphase with improper merotelic microtubule attachments. Accordingly, short-term treatment (<24 h) with small molecules that prolong mitotic duration or destabilize chromosome microtubule attachments reduces merotelic errors and lagging chromosome rates, although hPSCs adapt and lagging chromosome rates rebound upon long-term (>24 h) microtubule destabilization. Strikingly, we also demonstrate that mitotic error rates correlate with developmental potential decreasing or increasing upon loss or gain of pluripotency, respectively. Thus, a low mitotic fidelity is an inherent and conserved phenotype of hPSCs. Moreover, chromosome segregation fidelity depends on developmental state in normal human cells.

## INTRODUCTION

Human pluripotent stem cells (hPSCs), including embryonic and induced PSCs, can differentiate into cell types of all three embryonic germ layers and hence hold great promise for modeling and treating human diseases and conditions. However, during *in vitro* propagation, hPSCs often become aneuploid with incorrect numbers of chromosomes. Aneuploidy in hPSCs is attributed to culture adaptation that selects for stable aneuploid karyotypes, which outcompete diploid hPSCs, thus limiting therapeutic applications (Baker et al., 2007; Mayshar et al., 2010; Price et al., 2021; Taapken et al., 2011).

Although culture adaptation explains how reoccurring constitutive aneuploidies become dominant, it does not explain how or why mitotic chromosome segregation errors occur in hPSCs that generate the aneuploid genomes for selection to act upon. Perturbed DNA replication dynamics, DNA damage, and defects in chromosome condensation associated with structural aneuploidies involving copy-number alterations to chromosomal segments contribute to mitotic defects in hPSCs (Burrell et al., 2013; Halliwell et al., 2020; Lamm et al., 2016). However, aneuploidy due to the gain or loss of whole chromosomes is also frequent (Baker et al., 2007; Mayshar et al., 2010; Taapken et al., 2011), but we do not know the mitotic pathways responsible for whole-chromosome segregation errors in hPSCs.

Similarly, during early human embryogenesis, aneuploidy is prevalent in totipotent and pluripotent embryonic cells, with 25%–90% of *in vitro* fertilization (IVF) preimplantation human embryos being aneuploid irre-

spective of maternal age, infertility, or embryo quality (McCoy et al., 2015; Mertzaniidou et al., 2013; Starostik et al., 2020; Vanneste et al., 2009). Due to obvious legal and ethical restrictions, aneuploidy rates in naturally conceived human embryos are unknown but are thought to correspond to IVF preimplantation embryo rates accounting for only ~30% of conceptions resulting in live births (Macklon et al., 2002; McCoy, 2017), with aneuploidy being the leading cause of miscarriages and birth defects (Hassold and Hunt, 2001; Menasha et al., 2005).

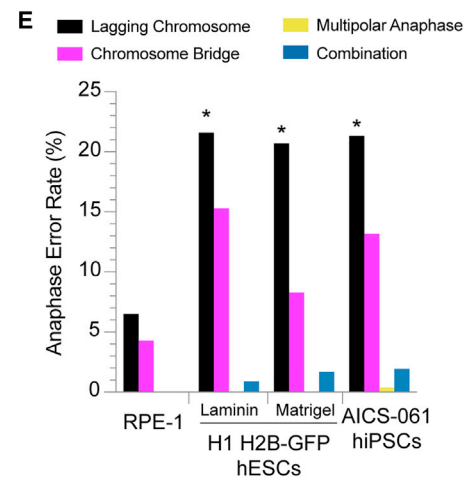
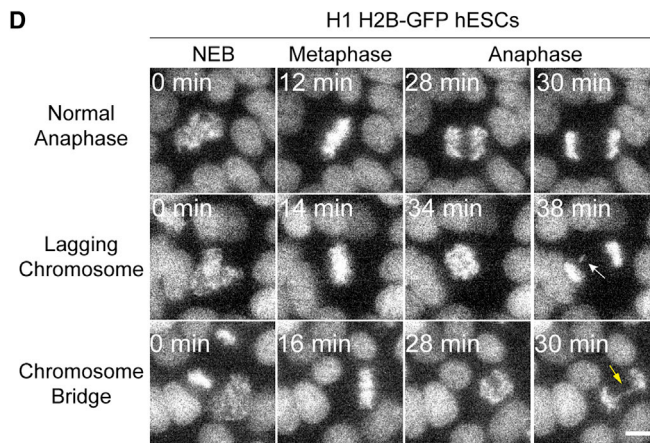
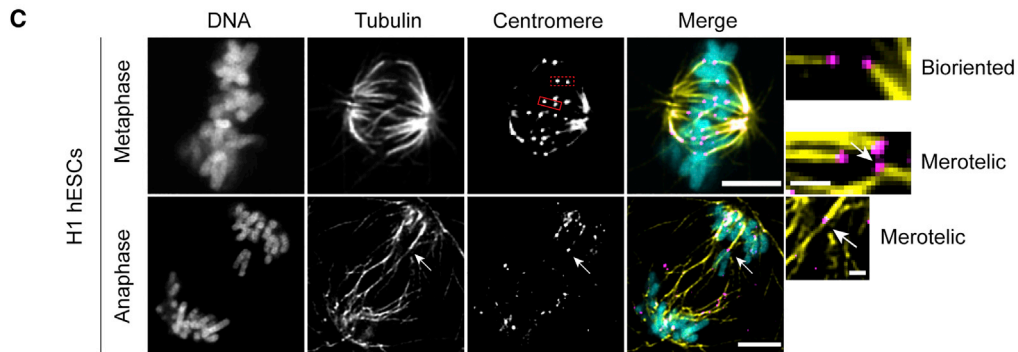
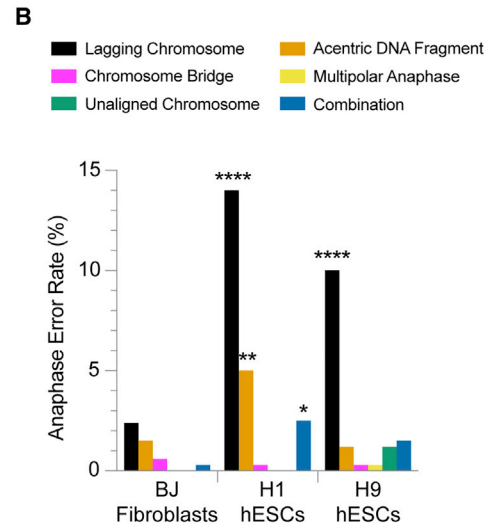
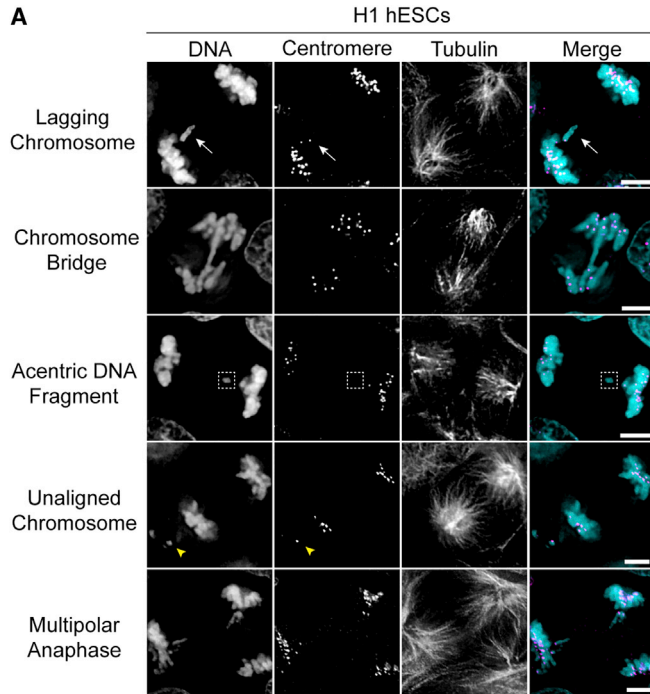
Surprisingly, like hPSCs, whole-chromosome abnormalities caused by mitotic errors are more frequent than meiotic errors and structural aneuploidies in IVF preimplantation embryos (McCoy et al., 2015; Starostik et al., 2020; Vanneste et al., 2009). This raises the possibility that mitotic errors and aneuploidy are intrinsic characteristics of pluripotent cells. Here, we investigate the mechanisms responsible for mitotic chromosome segregation errors and test the influence of mitotic duration, chromosome microtubule attachment stability, and developmental potential on chromosome segregation fidelity in hPSCs.

## RESULTS

### Mitotic error rates are increased in hPSCs compared with somatic cells

Initially, we quantified mitotic errors, focusing on anaphase errors, in pluripotent H1 and H9 human embryonic stem cells (hESCs) (Thomson et al., 1998) and normal, primary somatic BJ fibroblasts (Figures 1A and 1B). Lagging





(legend on next page)



chromosomes, unaligned chromosomes, and multipolar anaphases cause whole-chromosome aneuploidy, while acentric DNA fragments and chromosome bridges lead to structural aneuploidy (Figures 1A and 1B) (Burrell et al., 2013; Orr et al., 2015; Thompson and Compton, 2008). We also included a combination category for cells that exhibited multiple types of errors (Figures 1A and 1B).

In BJ fibroblasts, lagging chromosomes were the most frequent error, but the rate was less than 5% (Figure 1B), in agreement with the mitotic error and aneuploidy rates in other normal human somatic cells and tissues (Cimini et al., 1999; Knouse et al., 2014; Thompson and Compton, 2008). In comparison, the rate and relative proportion of mitotic errors caused by lagging chromosomes was significantly higher in H1 and H9 hESCs compared with BJ fibroblasts (Figure 1B; Table S1). H1, but not H9, hESCs also had a significantly higher frequency of acentric DNA fragments (Figure 1B), but these errors were less prevalent than lagging chromosomes. In parallel samples, we quantified that >95% of the H1 or the H9 population expressed the pluripotency transcription factors OCT4 or NANOG (Figures S1A and S1B), indicating that we measured the mitotic error rates of pluripotent cells.

In other mammalian and human cancer cells, lagging chromosomes are caused by the persistence of improper merotelic chromosome microtubule (or kinetochore microtubule [k-MT]) attachments with a chromosome simultaneously attached to microtubules from both spindle poles (Cimini et al., 2001; Thompson et al., 2010). Accordingly, we examined if hESCs exhibited lagging chromosomes with merotelic attachments. In metaphase, H1 and H9 hESCs had both correct bioriented (sister chromatids attached to microtubules from opposite spindle poles) and incorrect merotelic attachments (Figures 1C and S1C). Notably, 73% and 50% of lagging chromosomes in H1 and H9 hESCs, respectively, had merotelic attachments

(Figures 1C and S1C), but this is likely an underestimate because we could not always track microtubules back to their respective spindle poles. Furthermore, since hPSCs often become aneuploid (Baker et al., 2007; Mayshar et al., 2010; Taapken et al., 2011), which increases genomic instability (Passerini et al., 2016), in parallel, we karyotyped our H1 and H9 hESC lines to monitor their genomic stability because it is not readily feasible to simultaneously analyze the same cells for mitotic errors and determine their karyotype. For each, 20/20 cells scored were diploid, indicating with 95% confidence that less than 14% of cells in either population were aneuploid (Baker et al., 2016), arguing that some diploid H1 and H9 hESCs exhibit lagging chromosomes with merotelic attachments.

To further validate our findings, we performed time-lapse live-cell fluorescence microscopy with greater temporal resolution and sensitivity. We quantified errors in H2B-GFP expressing normal, immortalized somatic RPE-1 epithelial cells, H1 hESCs (Calder et al., 2013), and AICS-061 human induced pluripotent stem cells (hiPSCs) that were derived from parental WTC-11 hiPSCs (Hayashi et al., 2016) (Figures 1D and 1E; Videos S1, S2, and S3). In agreement, lagging chromosome rates were significantly elevated in H1 and AICS-061 hPSCs compared with RPE-1 cells (Figure 1E; Video S2). Although we cannot definitively distinguish acentric DNA fragments from lagging chromosomes in these experiments, we classified these errors as lagging chromosomes because of the low incidence of acentrics in our other analyses (Figures 1B, S3A, S3F, S3H, S4C, and S4E). Interestingly, in hPSCs, all lagging chromosomes re-incorporated into a main nucleus, and no micronuclei formed. Furthermore, H1 hESCs exhibited an increased lagging chromosome rate irrespective of whether cells were dissociated and seeded as single cells or aggregates on a Laminin-521 or a Matrigel matrix, respectively (Figure 1E). In contrast to somatic epithelial tissues (Knouse et al.,

### Figure 1. Lagging chromosome rates are increased in hPSCs compared with somatic cells

(A) Representative images of anaphase errors including a lagging chromosome with a centromere (white arrow), chromosome bridge, acentric DNA fragment lacking a centromere (box), unaligned chromosome with a centromere (yellow arrowhead), and multipolar anaphase in H1 hESCs. Shown are DNA (cyan), centromeres (magenta), and microtubules. Scale bars: 5  $\mu$ m.

(B) Percentage of anaphase errors in primary somatic BJ fibroblasts and H1 and H9 hESCs plated as single cells on Laminin-521.  $n > 250$  anaphases.

(C) Representative images of chromosome microtubule attachments in metaphase and anaphase H1 hESCs. Shown are DNA (cyan), microtubules (yellow), and centromeres (magenta). In the metaphase cell, shown is a bioriented (dashed box) or a merotelic attachment (solid box, white arrow). The anaphase cell shows a lagging chromosome with a merotelic attachment (white arrow). Insets are magnified views. Scale bars: 5  $\mu$ m (main) and 1  $\mu$ m (insets).

(D) Selected panels from live-cell imaging of H1 H2B-GFP hESCs showing a normal anaphase and anaphases with a lagging chromosome (white arrow) or chromosome bridge (yellow arrow). Scale bar: 10  $\mu$ m.

(E) Percentage of anaphase errors in somatic RPE-1 H2B-GFP cells, H1 H2B-GFP hESCs plated as single cells on Laminin-521 or as aggregates on Matrigel, and AICS-061 hiPSCs.  $n = 46$  anaphases in RPE-1 cells and  $n > 110$  anaphases in hPSCs.

At least three independent experiments (B and E); \* $p < 0.05$ , \*\* $p < 0.01$ , \*\*\* $p < 0.0001$  using a two-tailed Fisher exact test (B and E). See also Figure S1.

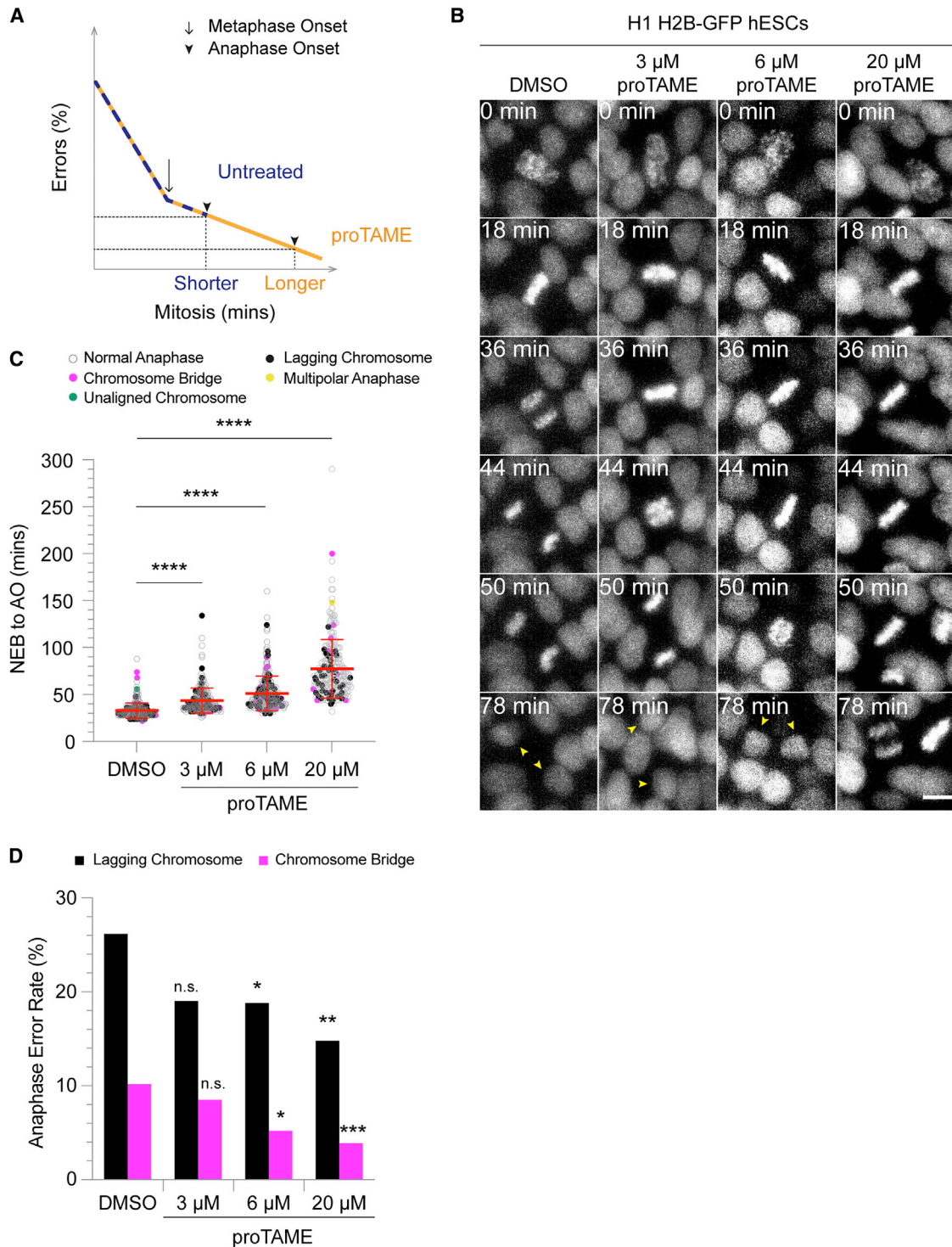


**Figure 2. Prolonging mitotic duration decreases mitotic error rates in hPSCs**

(A) Model illustrating the relationship between mitotic errors and mitotic duration. Early in mitosis, improper chromosome microtubule attachments are prevalent, but errors decline as mitosis progresses, and improper attachments are converted to correct ones. Prolonging mitosis using proTAME increases the amount of time for error correction, reducing the frequency of mitotic errors.

(B) Selected panels from live-cell imaging of H1 H2B-GFP hESCs that were treated with DMSO or increasing concentrations of proTAME (yellow arrowheads indicate daughter nuclei). Scale bar: 10  $\mu$ m.

(legend continued on next page)



2018), our results combined with the high incidence of mitotic errors in IVF preimplantation embryos (McCoy et al., 2015; Starostik et al., 2020; Vanneste et al., 2009), which maintain their 3D structure, argue that the disruption of tissue structure is unlikely to artificially increase mitotic error rates for hPSCs.

There was no significant difference in the chromosome bridge, multipolar anaphase, or unaligned chromosome rates between RPE-1 cells and hPSCs (Figure 1E). Furthermore, we observed an H1 hESC that delayed anaphase onset for >2 h due to a chromosome that failed to align (Figure S1D; Video S4), indicating that the spindle assembly checkpoint (SAC) (Musacchio and Salmon, 2007) is functional and responsive to unattached chromosomes in hPSCs. Collectively, our results agree with previous studies that quantified total mitotic error rates between 15%–20% in hPSCs (Halliwell et al., 2020; Lamm et al., 2016; Milagre et al., 2020; Zhang et al., 2019), but we extend these observations and demonstrate that both embryonic and induced PSCs exhibit an elevated mitotic error rate, due to lagging chromosomes with improper merotelic attachments, compared with somatic cells.

### Prolonging mitotic duration decreases mitotic error rates in hPSCs

Next, we investigated why lagging chromosomes with merotelic attachments are more prevalent in hPSCs compared with somatic cells and on testing strategies to reduce lagging chromosome rates because chromosome missegregation and lagging chromosome rates are proportional (Thompson and Compton, 2008). The SAC does not detect improper merotelic attachments (Cimini et al., 2001); rather, merotelic attachments are converted to correct bio-oriented attachments by kinases and microtubule depolymerases that facilitate iterative cycles of microtubule detachment and reattachment prior to anaphase onset (Godek et al., 2014). Thus, one parameter that influences merotelic error correction efficiency is mitotic duration. A longer duration allows for more cycles of microtubule detachment and reattachment decreasing errors and, conversely, a shorter duration increases errors (Figure 2A; note: error correction rate does not change). Accordingly, one hypothesis is that mitotic duration is shorter in hPSCs compared with somatic cells, hindering robust merotelic error correction and leading to an elevated frequency of lagging chromosomes. To test this hypothesis, we measured mitotic duration from nuclear envelope break-

down (NEB) to anaphase onset (AO) in H2B-GFP-expressing H1 hESCs, AICS-061 hiPSCs, and somatic RPE-1 cells by time-lapse live-cell fluorescent microscopy (Figure 1E). Mitotic duration (NEB to AO), including prometaphase (NEB to metaphase) and metaphase (metaphase to AO), was significantly increased in H1 and AICS-061 hPSCs compared with RPE-1 cells (Figure S1E), and there was no significant difference between hPSCs that went through a normal or an aberrant mitosis (Figure S1F), demonstrating that an insufficient mitotic duration is not responsible for the elevated lagging chromosome rates in hPSCs.

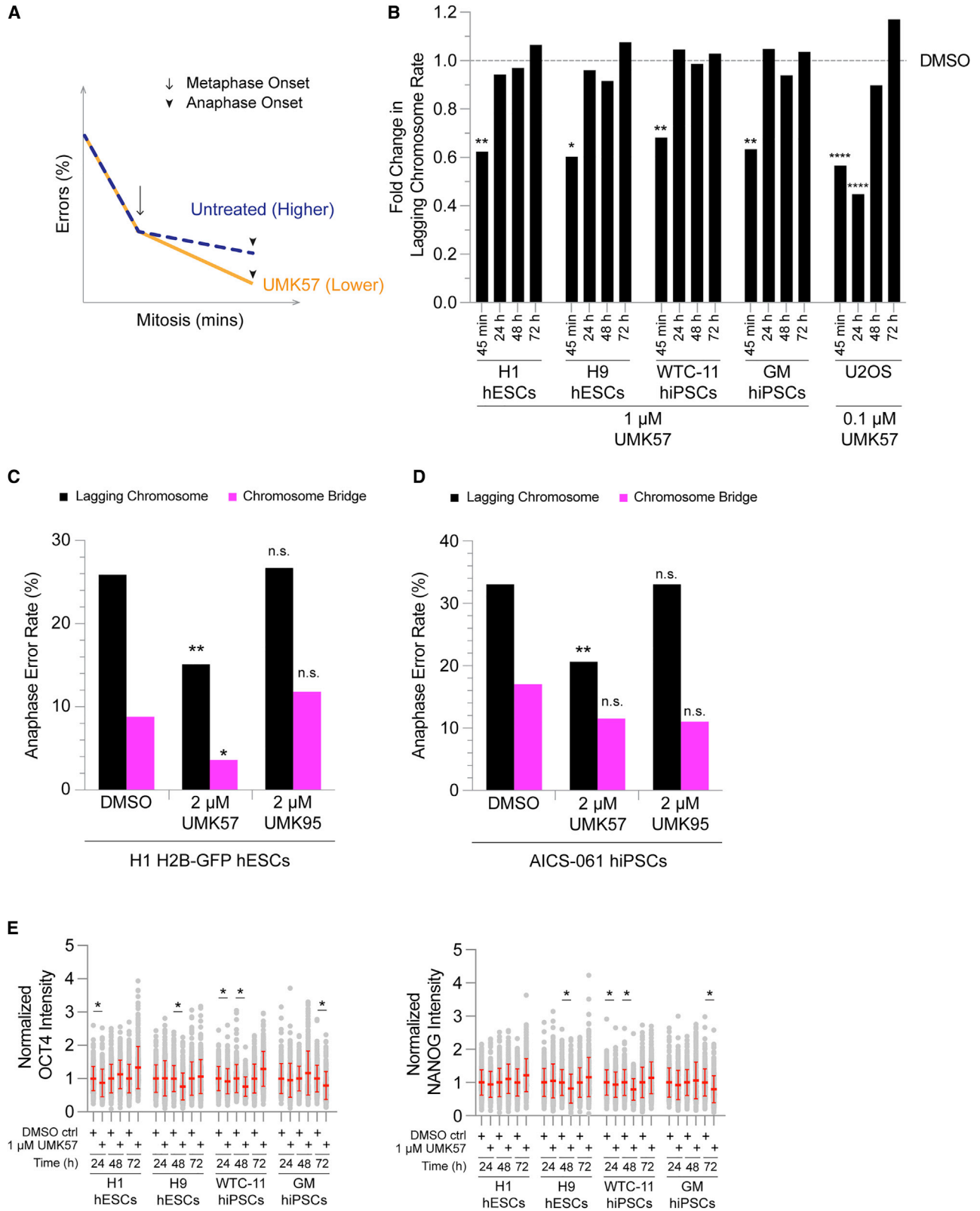
Nevertheless, we tested if prolonging mitosis reduces lagging chromosome rates in hPSCs by allowing for more cycles of microtubule release and reattachment prior to AO (Figure 2A). To test this strategy, we used the small molecule proTAME that inhibits the anaphase promoting complex/cyclosome (APC/C) E3 ubiquitin ligase and increases mitotic duration in somatic and cancer cells (Zeng et al., 2010). As a positive control, we reproduced previous results demonstrating that prolonging mitosis reduces the frequency of mitotic errors in RPE-1 cells when error rates are artificially elevated (Figures S2A–S2C) (Sansregret et al., 2017). For our experiments, we added proTAME to H1 or AICS-061 hPSCs immediately prior to performing live-cell imaging for 7 h. For these and subsequent experiments using small molecules, control conditions included 0.1% DMSO, but this does not affect lagging chromosome rates (Figure S2D). In parallel samples, we quantified that >95% of H1 or AICS-061 hPSCs expressed OCT4 or NANOG prior to proTAME treatment, indicating that we were analyzing pluripotent cells (Figures S2E and S2F).

For both H1 and AICS-061 hPSCs, mitotic duration significantly increased proportionally with proTAME concentration (Figures 2B, 2C, and S2G). Yet, the lagging chromosome rate significantly decreased only for H1 hESCs (Figures 2C, 2D, and S2I). Interestingly, metaphase was selectively lengthened proportional to proTAME concentration (Figure S2J) in H1 hESCs, similar to RPE-1 cells (Figure S2A), demonstrating that, at least for some cells, metaphase duration is a rate-limiting step in merotelic error correction. However, error correction is not exclusively determined by metaphase duration because although there was a significant decrease in metaphase duration for H1 hESCs that went through mitosis with a lagging chromosome versus normal mitosis with 20  $\mu$ M proTAME treatment, this did not occur with 6  $\mu$ M proTAME treatment (Figure S2K). Furthermore, chromosome bridges significantly decreased for H1 hESCs

---

(C and D) Mitotic duration (C) and percentage of lagging chromosomes or chromosome bridges (D) in H1 H2B-GFP hESCs treated with DMSO or proTAME.  $n \geq 250$  anaphases from six independent experiments; NEB, nuclear envelope breakdown; AO, anaphase onset; mean  $\pm$  SD (C); not significant (n.s.)  $p > 0.05$ , \* $p < 0.05$ , \*\* $p < 0.01$ , \*\*\* $p < 0.001$ , \*\*\*\* $p < 0.0001$  using a one-way ANOVA and Dunnett's multiple comparisons test (C) or a two-tailed Fisher exact test (D).

See also Figure S2.



(legend on next page)



(Figures 2C, 2D, and S2H) suggesting that prolonging mitosis also facilitates correction of these errors.

Since prolonging mitosis did not reduce the lagging chromosome rate in AICS-061 hiPSCs, we checked their genomic stability, reasoning that aneuploid cells could be insensitive to this strategy. There was a clonal abnormal karyotype with a terminal deletion of the long arm of chromosome 18 that occurred in only 10% (2/20) of the population and thus is unlikely to explain the different response. Also, we note that the lagging chromosome rate (~20%) is approximately double the frequency of aneuploid cells in the population, indicating that aneuploid cells do not solely account for the error rate. Combined, our results demonstrate that an abbreviated mitosis does not cause the high frequency of lagging chromosomes in hPSCs; however, prolonging mitosis, specifically metaphase, is an effective strategy to improve merotelic error correction and reduce lagging chromosome rates, albeit with the application limited to select hPSCs.

### Decreasing microtubule attachment stability reduces mitotic errors in hPSCs

The iterative cycles of microtubule detachment and reattachment required for merotelic error correction also dictate that the error correction rate depends on microtubule attachment turnover with hyperstable attachments (i.e., low turnover), inhibiting the release of incorrect merotelic attachments (Bakhom et al., 2009; Godek et al., 2014). Hence, hyperstable microtubule attachments in hPSCs relative to somatic cells is an alternative hypothesis explaining their elevated incidence of lagging chromosomes. This predicts that decreasing microtubule attachment stability (i.e., increasing turnover) will reduce lagging chromosome rates in hPSCs (Figure 3A; note: mitotic duration does not change). To test this prediction, we used the small molecule UMK57, an agonist of the microtubule depolymerase mitotic centromere-associated kinesin (MCAK, or KIF2C). In cancer cells with hyperstable attachments and high lagging chromosome rates, short-term UMK57 treatment destabi-

lizes microtubule attachments by potentiating MCAK activity, which reduces lagging chromosome rates. In contrast, somatic RPE-1 and BJ fibroblast cells with low rates of lagging chromosomes are insensitive to UMK57 (Orr et al., 2016). To test the effect of destabilizing microtubule attachments in hPSCs, we treated H1 and H9 hESCs and WTC-11 and GM hiPSCs for 45 min with UMK57 or the inactive analog UMK95 and subsequently measured anaphase error rates (Orr et al., 2016).

Short-term UMK57 treatment significantly reduced lagging chromosome rates in hPSCs and control U2OS cancer cells, while UMK95 treatment did not (Figures 3B and S3G). The reason higher concentrations of UMK57 were required to significantly reduce the lagging chromosome rate in hPSCs compared with U2OS cells is unknown. The rates of other errors were not reduced (Figure S3A), highlighting that distinct mechanisms are responsible for different types of mitotic errors, mitotic progression was not blocked (Figure S3B), and the hPSC populations expressed the pluripotency transcription factors OCT4 and NANOG (Figure S3E). Moreover, we performed these experiments using the same batch of H1 and H9 hESCs that we karyotyped during our analysis of microtubule attachments (Figures 1C and S1C) and showed were diploid. Combined, these results demonstrate that in hPSCs, destabilizing chromosome microtubule attachments reduces the frequency of lagging chromosomes (Figure 3A).

We modeled the effects of mitotic duration and microtubule attachment stability on merotelic error correction as independent pathways (Figures 2A and 3A), but these may influence error correction in a dependent manner. To test this, we simultaneously measured mitotic duration and errors in H1 H2B-GFP and AICS-061 hPSCs by time-lapse live-cell fluorescence microscopy in the presence of UMK57 for 12 h (Figures 3C, 3D, S3C, and S3D). As expected, UMK57 treatment significantly reduced lagging chromosome rates in H1 (Figure 3C) and AICS-061 hPSCs (Figure 3D), while UMK95 did not. Chromosome bridges were also significantly decreased in H1 hESCs (Figure 3C) but not in AICS-061

### Figure 3. Decreasing microtubule stability temporarily reduces mitotic error rates in hPSCs, but hPSCs rapidly adapt

(A) Model showing that higher microtubule attachment stability decreases the correction rate of improper attachments, while lowering microtubule attachment stability using UMK57 increases the correction rate reducing mitotic errors.

(B) Fold change in the lagging chromosome rate in H1, H9, WTC-11, and GM hPSCs and U2OS cancer cells after treatment with 1 or 0.1  $\mu$ M UMK57 for 45 min or 24, 48, or 72 h. For each cell line and time point, the lagging chromosome rate was normalized to a DMSO control for that time point;  $n > 300$  anaphases per condition.

(C and D) Percentage of lagging chromosomes and chromosome bridges from live-cell imaging of H1 H2B-GFP hESCs (C) or AICS-061 hiPSCs (D) treated with DMSO, 2  $\mu$ M UMK57, or 2  $\mu$ M UMK95 for 12 h.  $n > 150$  anaphases.

(E) Quantification of OCT4 and NANOG protein levels in H1, H9, WTC-11, and GM hPSCs in parallel samples from (B). Each time point was normalized to the corresponding DMSO control, and only conditions with significant decreases are marked.  $n = 300$  cells; mean  $\pm$  SD.

At least three independent experiments (B–E); n.s.  $p > 0.05$ , \* $p < 0.05$ , \*\* $p < 0.01$ , \*\*\*\* $p < 0.0001$  using a two-tailed Fisher's exact test (B–D); \* $p < 0.05$  using a two-tailed Student's t test (E).

See also Figure S3.



hiPSCs (Figure 3D). Interestingly, there was a significant increase in mitotic duration, metaphase specifically, with UMK57, but not with UMK95, treatment for both H1 and AICS-061 hPSCs (Figures S3C and S3D). However, for H1 hESCs, the increase in metaphase duration with UMK57 (8.2 min) was comparable to 3  $\mu$ M proTAME (11.5 min), which did not significantly reduce the lagging chromosome rate (Figure 2D). For AICS-061 hiPSCs, no delay in mitotic progression reduced the lagging chromosome rate (Figure S2I), suggesting that potentiating MCAK depolymerase activity predominantly enhances error correction by destabilizing microtubule attachments. Thus, mitotic duration and microtubule attachment stability are largely two independent parameters that influence merotelic error correction efficiency.

During these experiments, we monitored the genomic stability of H1 H2B-GFP and AICS-061 hPSCs. Similar to our previous analysis, <10% (3/32) of the AICS-061 hiPSCs had a clonal aneuploid karyotype. For H1 H2B-GFP hESCs, karyotyping performed after completing two experimental replicates found that 20/20 cells were diploid, while 25% (5/20) of cells had an interstitial duplication of the long arm of chromosome 20 after the third experimental replicate. Overall, the reduction in lagging chromosome rates upon short-term UMK57 treatment is reproducible using multiple hPSC lines, arguing that the low incidence of aneuploid cells is unlikely to influence the outcomes. Collectively, these results support our hypothesis that hyperstable chromosome microtubule attachments contribute to the elevated frequency of lagging chromosomes in hPSCs.

### hPSCs rapidly adapt to UMK57

We next investigated if UMK57 is an effective chemical strategy to reduce lagging chromosome rates in hPSCs upon long-term culturing. Cancer cells, including U2OS cells, rapidly adapt to UMK57, with microtubule attachment stability increasing and lagging chromosome rates rebounding after ~48 h (Orr et al., 2016). In contrast, somatic fibroblasts from aged donors that exhibit elevated lagging chromosome rates do not adapt upon long-term UMK57 treatment (Barroso-Vilares et al., 2020). We treated hPSCs or U2OS cells (a positive control for adaptation) with UMK57 for 24, 48, and 72 h. During the time course, media with UMK57 were replaced fresh daily. Surprisingly, by 24 h, there was no significant difference in lagging chromosome rates between DMSO control and either 1 or 2  $\mu$ M UMK57-treated hPSCs, and after 72 h, lagging chromosome rates were slightly elevated above baseline for almost all cell lines (Figures 3B and S3G). Also, there was no change in the rates of other mitotic errors (Figures S3F and S3H), and hPSCs continued to express the pluripotency transcription factors OCT4 and NANOG with only minor fluctuations in the levels (Figures 3E and S3I).

Thus, hPSCs rapidly adapt to UMK57 preserving a high lagging chromosome rate.

### Developmental potential influences mitotic error rates

Our repeated observations that mitotic error rates, and particularly lagging chromosomes, are elevated in hPSCs compared with somatic cells (Figures 1B and 1E) coupled with the high mitotic error rates in preimplantation human embryos (McCoy et al., 2015; Vanneste et al., 2009) led us to question whether a high error rate is an intrinsic and a cell autonomous trait linked to developmental state. This idea predicts that as developmental potential decreases or increases, mitotic error rates also decrease or increase, respectively (Figure 4A). We tested this prediction using isogenic cells with different developmental states to minimize genetic diversity as a confounding variable.

We compared mitotic error rates between isogenic primary somatic WTC or GM fibroblasts with parental WTC-11 and the derivative AICS-061 hiPSCs or GM hiPSCs (Brennan et al., 2011), respectively. Lagging chromosome rates were significantly elevated in hiPSCs compared with isogenic somatic fibroblasts (Figures 4B and S4C; Table S1). In addition, we karyotyped WTC fibroblasts and WTC-11 hiPSCs to confirm that abnormal aneuploid cells present in either population did not exclusively account for the error rates. WTC fibroblasts were diploid (20/20), while 10% (2/20) of the WTC-11 hiPSCs had a clonal balanced translocation between the short arm of chromosome 1 and the long arm of chromosome 16. As a hypothetical test, we assumed that all aneuploid WTC-11 hiPSCs go through an aberrant mitosis with a lagging chromosome, so we discarded the WTC-11 hiPSC lagging chromosome data attributed to the aneuploid cells in the population. After making this hypothetical adjustment, lagging chromosome rates remained significantly elevated in WTC-11 hiPSCs compared with WTC fibroblasts, arguing that aneuploid WTC-11 hiPSCs in the population cannot solely account for the error rate observed (Figure S4D). Furthermore, we quantified the percentage of cells expressing the pluripotency transcription factors OCT4 and NANOG, and as expected, somatic fibroblasts did not express OCT4 and NANOG, while hiPSCs did (Figures S4A and S4B). Thus, with increased developmental potential, mitotic error rates increase.

Conversely, differentiation and loss of pluripotency should decrease error rates according to our prediction. To test this, we induced undirected differentiation in H1 and H9 hESCs and WTC-11 and GM hiPSCs with all-*trans* retinoic acid (RA) (Jain et al., 2012). After 4 days of RA undirected differentiation, hPSCs acquired the morphology of differentiated cells (Figure S4F), and expression of the pluripotency transcription factors OCT4, NANOG, and SOX2 significantly decreased comparable to levels in somatic fibroblasts (Figures S5A–S5C), indicating loss of pluripotency. Although

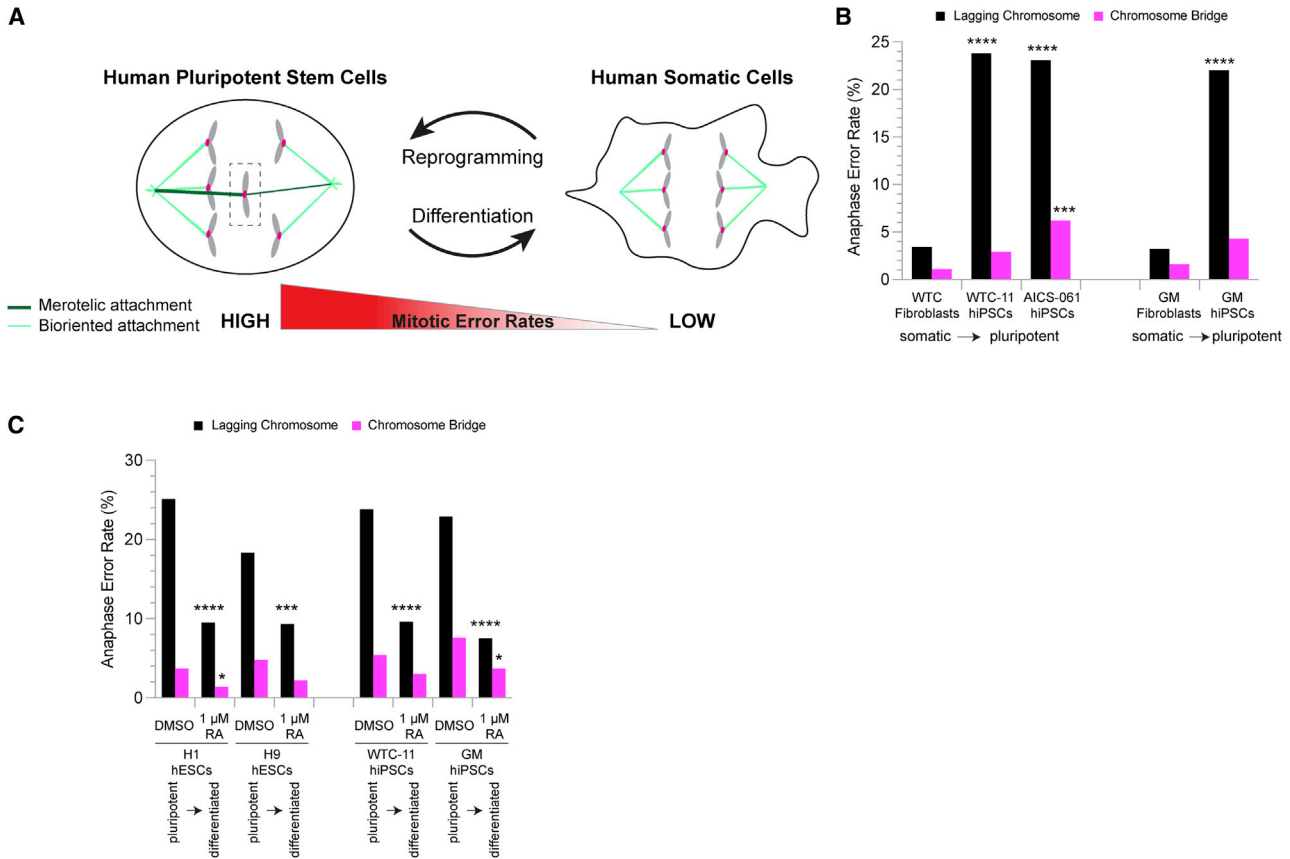


**Figure 4. Mitotic error rates correlate with developmental potential**

(A) Model showing that as developmental potential decreases or increases, mitotic errors also decrease or increase, respectively. (B) Percentage of lagging chromosomes and chromosome bridges in isogenic somatic WTC fibroblasts, WTC-11 hiPSCs, and AICS-061 hiPSCs (left) and isogenic GM fibroblasts and GM hiPSCs (right).  $n > 250$  anaphases. (C) Percentage of lagging chromosomes and chromosome bridges in H1 and H9 hESCs and WTC-11 and GM hiPSCs after 4 day treatment with DMSO or 1  $\mu$ M all-*trans* retinoic acid (RA) to induce undirected differentiation.  $n > 300$  anaphases. At least three independent experiments (B and C); \* $p < 0.05$ , \*\*\* $p < 0.001$ , \*\*\*\* $p < 0.0001$  using a two-tailed Fisher's exact test (B and C). See also [Figures S4](#) and [S5](#).

we observed a minor, but significant, increase, in multipolar anaphases ([Figure S4E](#)), lagging chromosome rates were significantly decreased by ~50% compared with DMSO control hPSCs ([Figure 4C](#)), demonstrating that decreasing developmental potential reduces mitotic error rates.

In mosaic mouse embryos and human gastruloids composed of diploid and aneuploid cells, aneuploid cells are depleted as development progress and differentiation occurs ([Bolton et al., 2016](#); [Yang et al., 2021](#)). Analogous to this is the possibility that aneuploid cells present in the starting hPSC populations used for the RA experiments are responsible for the mitotic errors but become depleted during differentiation, thus decreasing the error rate. This scenario requires that hPSC populations are composed of aneuploid cells or are mosaic populations of diploid and aneuploid cells. To test this, we karyotyped the H1 and the H9 hESC

populations after completion of all experimental replicates, reasoning that clonal and/or non-clonal aneuploidies were most likely to be detected after prolonged culturing. Critically, both the H1 and H9 populations were diploid (20/20), arguing that depletion of aneuploid cells during differentiation is unlikely to explain the decrease in errors. Collectively, our results show that mitotic error rates correlate with developmental potential and suggest that a high mitotic error rate is an inherent and cell-autonomous trait of hPSCs.

## DISCUSSION

Here, we show that lagging chromosomes in anaphase, caused by merotelic microtubule attachments, are the most frequent mitotic error in hPSCs ([Figure 5](#)).

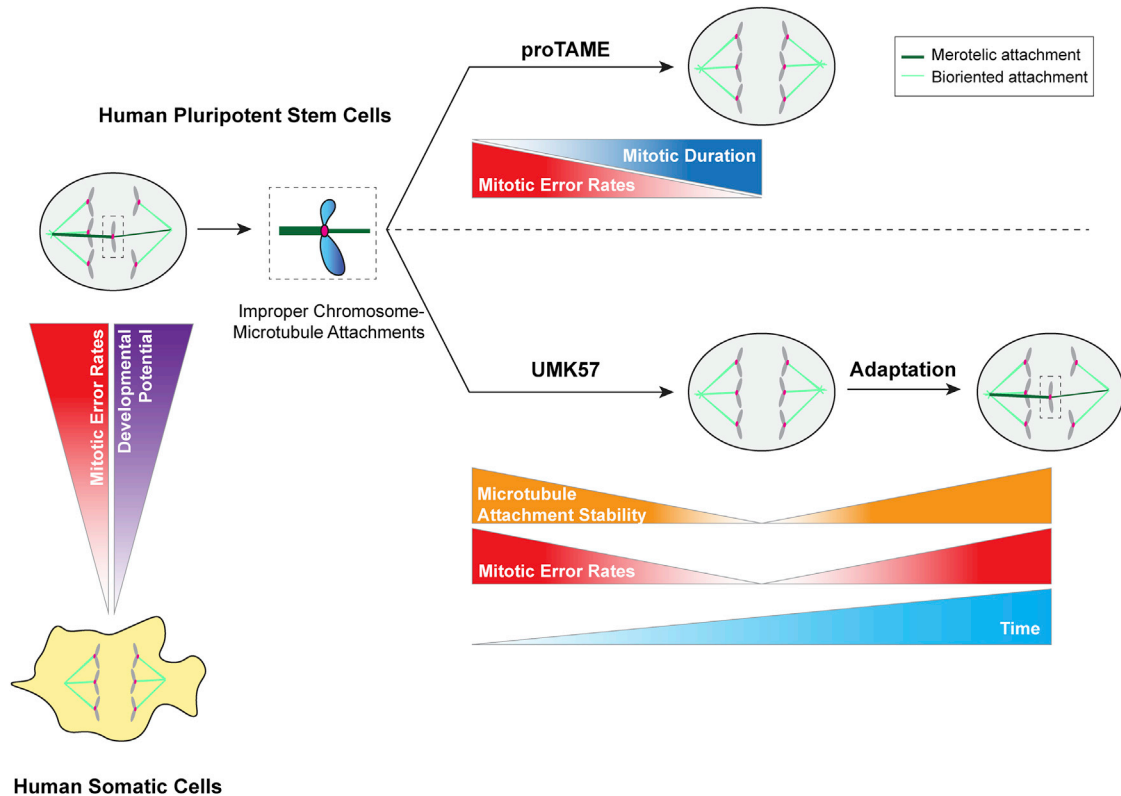


**Figure 5. Model illustrating the relationships between mitotic error rates and developmental potential, mitotic duration, and chromosome microtubule attachment stability**

We propose that mitotic error rates correlate with developmental potential such that the greater the developmental potency, the higher the mitotic error rate (left panel). Moreover, an elevated frequency of improper merotelic attachments underlies the lagging chromosome rate in hPSCs, and hence increasing mitotic duration or decreasing microtubule attachment stability improves merotelic error correction to reduce lagging chromosomes. However, hPSCs rapidly adapt to microtubule destabilization, restoring their high mitotic error rate (right panel).

Surprisingly, our results reveal that hPSCs are more similar to transformed cancer cells than normal somatic cells with respect to mitotic error rates (Cimini et al., 2001; Godek et al., 2016; Thompson and Compton, 2008). Furthermore, we show that mitotic error rates decrease or increase upon loss or gain of pluripotency, respectively, demonstrating that a high mitotic error rate is intrinsic to hPSCs (Figure 5). Moreover, multipotent neural stem cells exhibit an intermediate error rate (~10%) between hPSCs and somatic cells, suggesting that the mitotic error rate may scale linearly with developmental potential (Godek et al., 2016). Collectively, these results show that chromosome segregation fidelity is not universally conserved in normal human cells and that it depends on developmental state. This raises the possibility that in cancer cells, the (re)acquisition of a developmental program with greater potency causes an elevated mitotic error rate. This idea is further supported by the low frequency of mutations in mitotic genes found in cancer cells (Nath et al., 2015).

Assuming that chromosome missegregation and lagging chromosome rates are proportional in hPSCs, analogous to cancer cells (Thompson and Compton, 2008), then lagging chromosomes are a leading cause of aneuploidy in hPSCs. Ideally, we would directly measure chromosome missegregation rates, but the growth properties of hPSCs pose challenges to using conventional techniques (Godek and Compton, 2018). Regardless of the exact missegregation rate, these results delineate a pathway driving culture adaptation in hPSCs (Baker et al., 2007; Mayshar et al., 2010; Taapken et al., 2011). We propose that lagging chromosomes fuel culture adaptation, but this must also be coupled with the transient survival of aneuploid hPSCs, providing an opportunity for selection to occur (Figure S5D). Yet, we detect a low frequency of aneuploid hPSCs in culture, indicating that most aneuploid hPSCs are at a selective disadvantage. In this regard, hPSCs resemble somatic cells that exhibit cell-cycle arrest following chromosome missegregation (Thompson and Compton, 2010). In



contrast, cancer cells tolerate and propagate with aneuploid genomes (Godek et al., 2016; Thompson and Compton, 2010). How hPSCs gain an initial tolerance to an aneuploid genome for selection to act upon is unknown, but hPSCs acquire p53 mutations (Merkle et al., 2017), and this may lead to aneuploidy tolerance as shown in cancer cells (Thompson and Compton, 2010). Subsequently, selection for hPSCs with constitutive stable aneuploidies that support long-term survival and a growth advantage over diploid hPSCs occurs (Price et al., 2021). This multistep process also explains why culture adaptation often arises during extended propagation (Baker et al., 2007).

Given the potential consequence of generating aneuploid progeny from lagging chromosomes, understanding why merotelic attachments persist and devising strategies to reduce merotelic errors is paramount for the successful use of hPSCs in regenerative medicine. Here, we find that prolonging mitosis or destabilizing chromosome microtubule attachments using the small molecules proTAME or UMK57, respectively, improve merotelic error correction, reducing lagging chromosomes in hPSCs, albeit temporarily (Figure 5). We note that prolonging mitosis using proTAME also decreases the incidence of unaligned chromosomes during mouse preimplantation development, presumably by increasing attachment formation rather than merotelic error correction (Vázquez-Diez et al., 2019). Furthermore, our UMK57 results suggest that hyperstable microtubule attachments underlie the elevated frequency of lagging chromosomes in hPSCs and that hPSCs may rewire mitotic signaling networks to adapt to UMK57, preserving a high error rate (Figure 5) similar to cancer cells (Bakhoun et al., 2009; Orr et al., 2016). Direct measurement of microtubule attachment turnover rates in hPSCs will be necessary to test this. Although many molecular players regulating microtubule dynamics are known (Godek et al., 2014), how these networks differ between somatic cells or hPSCs and cancer cells is unknown. In contrast to aneuploid cancer cells, where genetic and transcriptional heterogeneity is a confounding variable (Zhao et al., 2019), hPSCs may offer a more tractable system to determine the molecular and signaling pathways promoting lagging chromosomes.

Extending our results to human preimplantation development suggests that lagging chromosomes are primarily responsible for mitotic errors in early embryonic cells, thus providing a mechanism for the whole-chromosome aneuploidy observed in preimplantation embryos (Figure S5E) (McCoy et al., 2015; Starostik et al., 2020; Vanneste et al., 2009). In support, lagging chromosomes occur during the first mitotic division in human embryos (Cavazza et al., 2021; Currie et al., 2022). In contrast, during mouse preimplantation development, unaligned chromosomes are the most frequent mitotic error (Vázquez-Diez et al., 2019). This difference may contribute

to the discrepancy in aneuploidy rates: ~5% mouse embryos (Lightfoot et al., 2006; Wei et al., 2011) versus 25%–90% human embryos (McCoy et al., 2015; Mertzani-dou et al., 2013; Starostik et al., 2020; Vanneste et al., 2009). Accordingly, this raises the question of how euploid human embryos are established to support normal development. Like most aneuploid hPSCs, aneuploid preimplantation embryonic cells may be at a selective disadvantage when in competition with diploid embryonic cells. In support, transferred mosaic IVF embryos composed of aneuploid and diploid cells can result in normal development and live births (Yang et al., 2021). Importantly, our results also suggest that declining mitotic error rates as developmental potential decreases upon differentiation support the establishment of euploid embryos (Figure S5E). Thus, during human development, genome stability is achieved because the time window comprising embryonic cells with high developmental potency and high mitotic error rates is limited. In contrast, the time window is unlimited for hPSCs growing in culture. In conclusion, our data support the view that in normal human cells, developmental state differentially influences the fidelity of chromosome segregation and the response to aneuploidy.

## EXPERIMENTAL PROCEDURES

### Resource availability

#### Corresponding author

The corresponding author is Kristina Godek (Kristina.M.Godek@dartmouth.edu).

#### Materials availability

Available from [corresponding author](#) upon request.

### Cell lines and cell culture

Primary BJ fibroblasts (CRL-2522), U2OS (HTB-96), and parental RPE-1 (CRL-4000) cells are available from the American Type Culture Collection. H1/WA01 and H9/WA09 hESCs are available from WiCell Research Institute. WTC-11 (GM25256) and GM (GM23476) hiPSCs and GM fibroblasts (GM04506) are available from the Coriell Institute for Medical Research. AICS-061 hiPSCs are available from the Allen Institute for Cell Science. H1 H2B-GFP hESCs were obtained from Dr. Jonathan Draper (McMaster University). WTC fibroblasts were obtained from the Gladstone Stem Cell Core.

In brief, all cell lines were cultured according to distributor protocols at 37°C in a humidified atmosphere with 5% CO<sub>2</sub> and routinely validated as mycoplasma free (Sigma-Aldrich Mycoplasma Kit #MP0035). A detailed list of reagents and protocols is in the [supplemental information](#). G-banded karyotyping was performed by WiCell Research Institute.

### Immunofluorescence

In brief, hPSCs were plated on either Matrigel- or Laminin-521-coated 18 mm glass coverslips. BJ, WTC, and GM fibroblasts and



U2OS cells were plated on standard 18 mm glass coverslips. For immunofluorescence, cells were fixed with either 3.5% paraformaldehyde or ice-cold methanol dependent on the antibodies. Following fixation, cells were permeabilized and blocked using Triton X-100 and 2% BSA. Subsequently, samples were incubated with primary antibodies, washed, and then incubated with fluorescent secondary antibodies and DAPI. Samples were then washed and mounted on glass slides using ProLong Gold antifade (Thermo Fisher Scientific #P36934).

To assess chromosome microtubule attachments, cells were pre-extracted with calcium buffer, fixed with 1% glutaraldehyde, and then quenched with 1 mg/mL sodium borohydride, followed by permeabilization and blocking with BSA and Triton X-100 prior to performing standard immunostaining. A detailed list of antibodies and protocols is in the [supplemental information](#).

### Microscopy

Images were acquired with a Hamamatsu ORCA-Fusion Gen III sCMOS camera on a Nikon Eclipse Ti2E, an Andor cooled CCD camera on a Nikon Eclipse Ti, or an Andor CSU-W1 two-camera spinning disk module, an Andor Zyla sCMOS camera, and an Andor ILE laser module on a Nikon Eclipse Ti. Objectives included Nipons CFI Plan Apo Lambda 60 $\times$ , 1.4 numerical aperture (NA) oil immersion (OI); CFI Super Plan Fluor LWD 20 $\times$  AMD, 0.7 NA air; Plan Apo VC 60 $\times$ , 1.4 NA OI; and Plan Apo Lambda 60 $\times$ , 1.4 NA OI. Z-step size was either 0.2, 0.5, or 1  $\mu$ m. For quantification of proteins, all images were acquired with the same acquisition parameters and exposure times. Additional details are in the [supplemental information](#).

Live-cell imaging was performed in modified rose chambers (RPE-1 H2B-GFP) or on 35 mm glass-bottom dishes (MatTek #P35G-1.5-14-C) coated with Matrigel or Laminin-521 (hPSCs) at 37°C in a humidified environment with 5% CO<sub>2</sub> (Tokai Hit Stage-top Incubation System) using the microscopes described above with binning set to 2  $\times$  2. Additional details are in the [supplemental information](#).

### Drug treatments

Cells were treated with 0.1% DMSO, UMK57 (Dr. Benjamin Kwok, University of Montreal, or Aobios #AOB8668) or UMK95 (Dr. Benjamin Kwok, University of Montreal) at the concentrations and times specified. For live-cell imaging, hPSCs were cultured in phenol-free mTeSR1 with 0.1% DMSO, proTAME (Tocris #I-440-01M), UMK57, or UMK95. RPE-1 H2B-GFP cells were cultured in phenol-free media supplemented with 0.1% DMSO or proTAME or arrested in 100  $\mu$ M monastrol (Tocris #1305) for 6 h, followed by washout with phenol-free media into 0.1% DMSO or proTAME. For all-*trans* RA differentiation assay, hPSCs were grown in mTeSR1 for 24 h, and then 1  $\mu$ M RA (Sigma #R2625) and fresh media were added daily for 4 days. Additional details are in the [supplemental information](#).

### Statistics

GraphPad Prism was used for all statistics. The statistical tests used, corresponding *n* values, error bar measurements, and *p* values are in the figure legends. No outliers were excluded.

## SUPPLEMENTAL INFORMATION

Supplemental information can be found online at <https://doi.org/10.1016/j.stemcr.2022.12.008>.

## AUTHOR CONTRIBUTIONS

Conceptualization, K.M.G.; methodology, K.M.G., C.D., and A.Y.; validation, K.M.G., C.D., and A.Y.; formal analysis, K.M.G., C.D., and A.Y.; investigation, K.M.G., C.D., and A.Y.; resources, K.M.G. and D.A.C.; writing – original draft, K.M.G. and C.D.; writing – review & editing, K.M.G., C.D., D.A.C., and A.Y.; visualization, K.M.G. and C.D.; supervision, K.M.G.; funding acquisition, K.M.G. and D.A.C.

## ACKNOWLEDGMENTS

We thank Jonathan Draper, Aaron Straight, Bruce Conklin, Benjamin Kwok, Thorsten Schlaeger, and Ann Lavanway for providing reagents or technical advice. Also, we thank Godek and Compton lab members for their helpful discussions, particularly Thomas Kucharski. This work was supported by National Institutes of Health GM051542 to D.A.C. and R01HD101436 to K.M.G. and a Hitchcock Foundation grant to K.M.G.

## CONFLICT OF INTERESTS

The authors declare no competing interests.

Received: January 31, 2022

Revised: December 9, 2022

Accepted: December 12, 2022

Published: January 12, 2023

## REFERENCES

- Baker, D., Hirst, A.J., Gokhale, P.J., Juarez, M.A., Williams, S., Wheeler, M., Bean, K., Allison, T.F., Moore, H.D., Andrews, P.W., et al. (2016). Detecting genetic mosaicism in cultures of human pluripotent stem cells. *Stem Cell Rep.* 7, 998–1012. <https://doi.org/10.1016/j.stemcr.2016.10.003>.
- Baker, D.E.C., Harrison, N.J., Maltby, E., Smith, K., Moore, H.D., Shaw, P.J., Heath, P.R., Holden, H., and Andrews, P.W. (2007). Adaptation to culture of human embryonic stem cells and oncogenesis in vivo. *Nat. Biotechnol.* 25, nbt1285. <https://doi.org/10.1038/nbt1285>.
- Bakhom, S.F., Genovese, G., and Compton, D.A. (2009). Deviant kinetochore microtubule dynamics underlie chromosomal instability. *Curr. Biol.* 19, 1937–1942. <https://doi.org/10.1016/j.cub.2009.09.055>.
- Barroso-Vilares, M., Macedo, J.C., Reis, M., Warren, J.D., Compton, D., and Logarinho, E. (2020). Small-molecule inhibition of aging-associated chromosomal instability delays cellular senescence. *EMBO Rep.* 21, e49248. <https://doi.org/10.15252/embr.201949248>.
- Bolton, H., Graham, S.J.L., Van der Aa, N., Kumar, P., Theunis, K., Fernandez Gallardo, E., Voet, T., and Zernicka-Goetz, M. (2016). Mouse model of chromosome mosaicism reveals lineage-specific depletion of aneuploid cells and normal developmental potential. *Nat. Commun.* 7, 11165. <https://doi.org/10.1038/ncomms11165>.



- Brennand, K.J., Simone, A., Jou, J., Gelboin-Burkhart, C., Tran, N., Sangar, S., Li, Y., Mu, Y., Chen, G., Yu, D., et al. (2011). Modelling schizophrenia using human induced pluripotent stem cells. *Nature* 473, 221–225. <https://doi.org/10.1038/nature09915>.
- Burrell, R.A., McClelland, S.E., Endesfelder, D., Groth, P., Weller, M.-C., Shaikh, N., Domingo, E., Kanu, N., Dewhurst, S.M., Gronroos, E., et al. (2013). Replication stress links structural and numerical cancer chromosomal instability. *Nature* 494, 492–496. <https://doi.org/10.1038/nature11935>.
- Calder, A., Roth-Albin, I., Bhatia, S., Pilquill, C., Lee, J.H., Bhatia, M., Levadoux-Martin, M., McNicol, J., Russell, J., Collins, T., et al. (2013). Lengthened G1 phase indicates differentiation status in human embryonic stem cells. *Stem Cells Dev.* 22, 279–295. <https://doi.org/10.1089/scd.2012.0168>.
- Cavazza, T., Takeda, Y., Politi, A.Z., Aushev, M., Aldag, P., Baker, C., Choudhary, M., Bucevičius, J., Lukinavičius, G., Elder, K., et al. (2021). Parental genome unification is highly error-prone in mammalian embryos. *Cell* 184, 2860–2877.e22. <https://doi.org/10.1016/j.cell.2021.04.013>.
- Cimini, D., Tanzarella, C., and Degrossi, F. (1999). Differences in malsegregation rates obtained by scoring ana-telophases or binucleate cells. *Mutagenesis* 14, 563–568. <https://doi.org/10.1093/mutage/14.6.563>.
- Cimini, D., Howell, B., Maddox, P., Khodjakov, A., Degrossi, F., and Salmon, E.D. (2001). Merotelic kinetochore orientation is a major mechanism of aneuploidy in mitotic mammalian tissue cells. *J. Cell Biol.* 153, 517–528. <https://doi.org/10.1083/jcb.153.3.517>.
- Currie, C.E., Ford, E., Benham Whyte, L., Taylor, D.M., Mihalas, B.P., Erent, M., Marston, A.L., Hartshorne, G.M., and McAinsh, A.D. (2022). The first mitotic division of human embryos is highly error prone. *Nat. Commun.* 13, 6755. <https://doi.org/10.1038/s41467-022-34294-6>.
- Godek, K.M., and Compton, D.A. (2018). Quantitative methods to measure aneuploidy and chromosomal instability. *Methods Cell Biol.* 144, 15–32. <https://doi.org/10.1016/bs.mcb.2018.03.002>.
- Godek, K.M., Kabeche, L., and Compton, D.A. (2014). Regulation of kinetochore–microtubule attachments through homeostatic control during mitosis. *Nat. Rev. Mol. Cell Biol.* 16, 57–64. <https://doi.org/10.1038/nrm3916>.
- Godek, K.M., Venere, M., Wu, Q., Mills, K.D., Hickey, W.F., Rich, J.N., and Compton, D.A. (2016). Chromosomal instability affects the tumorigenicity of glioblastoma tumor-initiating cells. *Cancer Discov.* 6, 532–545. <https://doi.org/10.1158/2159-8290.CD-15-1154>.
- Halliwell, J.A., Frith, T.J.R., Laing, O., Price, C.J., Bower, O.J., Stavish, D., Gokhale, P.J., Hewitt, Z., El-Khamisy, S.F., Barbaric, I., et al. (2020). Nucleosides rescue replication-mediated genome instability of human pluripotent stem cells. *Stem Cell Rep.* 14, 1009–1017. <https://doi.org/10.1016/j.stemcr.2020.04.004>.
- Hassold, T., and Hunt, P. (2001). To err (meiotically) is human: the genesis of human aneuploidy. *Nat. Rev. Genet.* 2, 280–291. <https://doi.org/10.1038/35066065>.
- Hayashi, Y., Hsiao, E.C., Sami, S., Lancero, M., Schlieve, C.R., Nguyen, T., Yano, K., Nagahashi, A., Ikeya, M., Matsumoto, Y., et al. (2016). BMP-SMAD-ID promotes reprogramming to pluripotency by inhibiting p16/INK4A-dependent senescence. *Proc. Natl. Acad. Sci. USA* 113, 13057–13062. <https://doi.org/10.1073/pnas.1603668113>.
- Jain, A.K., Allton, K., Iacovino, M., Mahen, E., Milczarek, R.J., Zwaka, T.P., Kyba, M., and Barton, M.C. (2012). p53 regulates cell cycle and MicroRNAs to promote differentiation of human embryonic stem cells. *PLoS Biol.* 10, e1001268. <https://doi.org/10.1371/journal.pbio.1001268>.
- Knouse, K.A., Wu, J., Whittaker, C.A., and Amon, A. (2014). Single cell sequencing reveals low levels of aneuploidy across mammalian tissues. *Proc. Natl. Acad. Sci. USA* 111, 13409–13414. <https://doi.org/10.1073/pnas.1415287111>.
- Knouse, K.A., Lopez, K.E., Bachofner, M., and Amon, A. (2018). Chromosome segregation fidelity in epithelia requires tissue architecture. *Cell* 175, 200–211.e13. <https://doi.org/10.1016/j.cell.2018.07.042>.
- Lamm, N., Ben-David, U., Golan-Lev, T., Storchová, Z., Benvenisty, N., and Kerem, B. (2016). Genomic instability in human pluripotent stem cells arises from replicative stress and chromosome condensation defects. *Cell Stem Cell* 18, 253–261. <https://doi.org/10.1016/j.stem.2015.11.003>.
- Lightfoot, D.A., Kouznetsova, A., Mahdy, E., Wilbertz, J., and Höög, C. (2006). The fate of mosaic aneuploid embryos during mouse development. *Dev. Biol.* 289, 384–394. <https://doi.org/10.1016/j.ydbio.2005.11.001>.
- Macklon, N.S., Geraedts, J.P.M., and Fauser, B.C.J.M. (2002). Conception to ongoing pregnancy: the “black box” of early pregnancy loss. *Hum. Reprod. Update* 8, 333–343. <https://doi.org/10.1093/humupd/8.4.333>.
- Mayshar, Y., Ben-David, U., Lavon, N., Biancotti, J.-C., Yakir, B., Clark, A.T., Plath, K., Lowry, W.E., and Benvenisty, N. (2010). Identification and classification of chromosomal aberrations in human induced pluripotent stem cells. *Cell Stem Cell* 7, 521–531. <https://doi.org/10.1016/j.stem.2010.07.017>.
- McCoy, R.C. (2017). Mosaicism in preimplantation human embryos: when chromosomal abnormalities are the norm. *Trends Genet.* 33, 448–463. <https://doi.org/10.1016/j.tig.2017.04.001>.
- McCoy, R.C., Demko, Z.P., Ryan, A., Banjevic, M., Hill, M., Sigurjonsson, S., Rabinowitz, M., and Petrov, D.A. (2015). Evidence of selection against complex mitotic-origin aneuploidy during preimplantation development. *PLoS Genet.* 11, e1005601. <https://doi.org/10.1371/journal.pgen.1005601>.
- Menasha, J., Levy, B., Hirschhorn, K., and Kardon, N.B. (2005). Incidence and spectrum of chromosome abnormalities in spontaneous abortions: new insights from a 12-year study. *Genet. Med.* 7, 251–263. <https://doi.org/10.1097/01.GIM.0000160075.96707.04>.
- Merkle, F.T., Ghosh, S., Kamitaki, N., Mitchell, J., Avior, Y., Mello, C., Kashin, S., Mekhoubad, S., Ilic, D., Charlton, M., et al. (2017). Human pluripotent stem cells recurrently acquire and expand dominant negative P53 mutations. *Nature* 545, 229–233. <https://doi.org/10.1038/nature22312>.
- Mertzanidou, A., Wilton, L., Cheng, J., Spits, C., Vanneste, E., Moreau, Y., Vermeesch, J.R., and Sermon, K. (2013). Microarray analysis reveals abnormal chromosomal complements in over 70% of 14 normally developing human embryos. *Hum. Reprod.* 28, 256–264. <https://doi.org/10.1093/humrep/des362>.



- Milagre, I., Pereira, C., Oliveira, R.A., and Jansen, L.E.T. (2020). Reprogramming of human cells to pluripotency induces CENP-A chromatin depletion. *Open Biol.* *10*, 200227. <https://doi.org/10.1098/rsob.200227>.
- Musacchio, A., and Salmon, E.D. (2007). The spindle-assembly checkpoint in space and time. *Nat. Rev. Mol. Cell Biol.* *8*, 379–393. <https://doi.org/10.1038/nrm2163>.
- Nath, S., Ghatak, D., Das, P., and Roychoudhury, S. (2015). Transcriptional control of mitosis: deregulation and cancer. *Front. Endocrinol.* *6*, 60. <https://doi.org/10.3389/fendo.2015.00060>.
- Orr, B., Godek, K.M., and Compton, D. (2015). Aneuploidy. *Curr. Biol.* *25*, R538–R542. <https://doi.org/10.1016/j.cub.2015.05.010>.
- Orr, B., Talje, L., Liu, Z., Kwok, B.H., and Compton, D.A. (2016). Adaptive resistance to an inhibitor of chromosomal instability in human cancer cells. *Cell Rep.* *17*, 1755–1763. <https://doi.org/10.1016/j.celrep.2016.10.030>.
- Passerini, V., Ozeri-Galai, E., de Pagter, M.S., Donnelly, N., Schmalbrock, S., Kloosterman, W.P., Kerem, B., and Storchová, Z. (2016). The presence of extra chromosomes leads to genomic instability. *Nat. Commun.* *7*, 10754. <https://doi.org/10.1038/ncomms10754>.
- Price, C.J., Stavish, D., Gokhale, P.J., Stevenson, B.A., Sargeant, S., Lacey, J., Rodriguez, T.A., and Barbaric, I. (2021). Genetically variant human pluripotent stem cells selectively eliminate wild-type counterparts through YAP-mediated cell competition. *Dev. Cell* *56*, 2455–2470.e10. <https://doi.org/10.1016/j.devcel.2021.07.019>.
- Sansregret, L., Patterson, J.O., Dewhurst, S., López-García, C., Koch, A., McGranahan, N., Chao, W.C.H., Barry, D.J., Rowan, A., Instrell, R., et al. (2017). APC/C dysfunction limits excessive cancer chromosomal instability. *Cancer Discov.* *7*, 218–233. <https://doi.org/10.1158/2159-8290.CD-16-0645>.
- Starostik, M.R., Sosina, O.A., and McCoy, R.C. (2020). Single-cell analysis of human embryos reveals diverse patterns of aneuploidy and mosaicism. *Genome Res.* *30*, 814–825. <https://doi.org/10.1101/gr.262774.120>.
- Taapken, S.M., Nisler, B.S., Newton, M.A., Sampsel-Barron, T.L., Leonhard, K.A., McIntire, E.M., and Montgomery, K.D. (2011). Karyotypic abnormalities in human induced pluripotent stem cells and embryonic stem cells. *Nat. Biotechnol.* *29*, 313–314. <https://doi.org/10.1038/nbt.1835>.
- Thompson, S.L., and Compton, D.A. (2008). Examining the link between chromosomal instability and aneuploidy in human cells. *J. Cell Biol.* *180*, 665–672. <https://doi.org/10.1083/jcb.200712029>.
- Thompson, S.L., and Compton, D.A. (2010). Proliferation of aneuploid human cells is limited by a p53-dependent mechanism. *J. Cell Biol.* *188*, 369–381. <https://doi.org/10.1083/jcb.200905057>.
- Thompson, S.L., Bakhoun, S.F., and Compton, D.A. (2010). Mechanisms of chromosomal instability. *Curr. Biol.* *20*, R285–R295. <https://doi.org/10.1016/j.cub.2010.01.034>.
- Thomson, J.A., Itskovitz-Eldor, J., Shapiro, S.S., Waknitz, M.A., Swiergiel, J.J., Marshall, V.S., and Jones, J.M. (1998). Embryonic stem cell lines derived from human blastocysts. *Science* *282*, 1145–1147. <https://doi.org/10.1126/science.282.5391.1145>.
- Vanneste, E., Voet, T., Le Caignec, C., Ampe, M., Konings, P., Melotte, C., Debrock, S., Amyere, M., Vikkula, M., Schuit, F., et al. (2009). Chromosome instability is common in human cleavage-stage embryos. *Nat. Med.* *15*, 577–583. <https://doi.org/10.1038/nm.1924>.
- Vázquez-Diez, C., Paim, L.M.G., and FitzHarris, G. (2019). Cell-size-independent spindle checkpoint failure underlies chromosome segregation error in mouse embryos. *Curr. Biol.* *29*, 865–873.e3. <https://doi.org/10.1016/j.cub.2018.12.042>.
- Wei, Y., Multi, S., Yang, C.-R., Ma, J., Zhang, Q.-H., Wang, Z.-B., Li, M., Wei, L., Ge, Z.-J., Zhang, C.-H., et al. (2011). Spindle assembly checkpoint regulates mitotic cell cycle progression during preimplantation embryo development. *PLoS One* *6*, e21557. <https://doi.org/10.1371/journal.pone.0021557>.
- Yang, M., Rito, T., Metzger, J., Naftaly, J., Soman, R., Hu, J., Albertini, D.F., Barad, D.H., Brivanlou, A.H., and Gleicher, N. (2021). Depletion of aneuploid cells in human embryos and gastruloids. *Nat. Cell Biol.* *23*, 314–321. <https://doi.org/10.1038/s41556-021-00660-7>.
- Zeng, X., Sigoillot, F., Gaur, S., Choi, S., Pfaff, K.L., Oh, D.C., Hathaway, N., Dimova, N., Cuny, G.D., and King, R.W. (2010). Pharmacologic inhibition of the anaphase-promoting complex induces a spindle checkpoint-dependent mitotic arrest in the absence of spindle damage. *Cancer Cell* *18*, 382–395. <https://doi.org/10.1016/j.ccr.2010.08.010>.
- Zhang, J., Hirst, A.J., Duan, F., Qiu, H., Huang, R., Ji, Y., Bai, L., Zhang, F., Robinson, D., Jones, M., et al. (2019). Anti-apoptotic mutations desensitize human pluripotent stem cells to mitotic stress and enable aneuploid cell survival. *Stem Cell Rep.* *12*, 557–571. <https://doi.org/10.1016/j.stemcr.2019.01.013>.
- Zhao, Y., Carter, R., Natarajan, S., Varn, F.S., Compton, D.A., Gawad, C., Cheng, C., and Godek, K.M. (2019). Single-cell RNA sequencing reveals the impact of chromosomal instability on glioblastoma cancer stem cells. *BMC Med. Genomics* *12*, 79. <https://doi.org/10.1186/s12920-019-0532-5>.